

## Dynamics and microscopic origin of fast 1.5 $\mu\text{m}$ emission in Er-doped $\text{SiO}_2$ sensitized with Si nanocrystals

S. Saeed,\* D. Timmerman, and T. Gregorkiewicz

*Van der Waals–Zeeman Institute, University of Amsterdam, Science Park 904, NL-1098 XH Amsterdam, The Netherlands*

(Received 30 November 2010; revised manuscript received 14 March 2011; published 27 April 2011)

We investigate the origin of fast 1.5  $\mu\text{m}$  photoluminescence from Er-doped  $\text{SiO}_2$  sensitized with silicon nanocrystals, which appears and decays within the first microsecond after a short laser excitation pulse. Time-resolved and temperature-dependent measurements on the 1.5  $\mu\text{m}$  emission from Er-doped and Er-free samples reveal that the major part of this emission is Er related. A possible contribution from other photoluminescence bands, specifically of the defect-related band centered around 1.3  $\mu\text{m}$ , has also been considered. All the results obtained indicate the dominant contribution of  $\text{Er}^{3+}$  ions to the fast 1.5  $\mu\text{m}$  emission in the investigated materials. We propose two possible mechanisms behind the fast excitation and quenching of  $\text{Er}^{3+}$  1.5  $\mu\text{m}$  emission, which are both facilitated by Er-related trap centers with ionization energy of  $E_A \approx 60$  meV.

DOI: [10.1103/PhysRevB.83.155323](https://doi.org/10.1103/PhysRevB.83.155323)

PACS number(s): 78.67.Bf, 31.70.Hq, 78.47.jd, 76.30.Kg

### I. INTRODUCTION

Rare-earth-doped materials have been investigated for a number of years in order to develop practical light sources for photonic applications. Among such materials Er-doped crystalline Si (*c*-Si:Er) was believed to be a promising system where the most advanced and successful Si technology could be used to manufacture optical elements whose emission coincides with the 1.5  $\mu\text{m}$  minimum absorption band of silica fibers used in telecommunications. Upon investigation, *c*-Si:Er emerged as a difficult material both to understand and in engineering.<sup>1,2</sup> Then a new approach of doping the  $\text{SiO}_2$  matrix with  $\text{Er}^{3+}$  ions and silicon nanocrystals (SiNCs) was proposed. It is now well established that there exists a strong interaction between SiNCs and  $\text{Er}^{3+}$  ions in a  $\text{SiO}_2$  matrix.<sup>3–7</sup> In such materials, upon illumination, light is initially absorbed by the SiNCs due to their large absorption cross section in the visible region.<sup>8</sup> The absorbed energy is then transferred to the  $\text{Er}^{3+}$  ions located inside and in the vicinity of the SiNCs, taking these ions to excited states. In this way an indirect excitation channel of  $\text{Er}^{3+}$  ions dispersed in  $\text{SiO}_2$  is created and 1.5  $\mu\text{m}$  emission appears, as the  $\text{Er}^{3+}$  ions relax from  $^4I_{13/2}$  back to the  $^4I_{15/2}$  ground state. This nonresonant  $\text{Er}^{3+}$  ion excitation has an effective excitation cross section of  $10^{-17}$ – $10^{-16}$   $\text{cm}^2$ , which represents an increase by a factor of  $10^3$  in comparison to the resonant pumping of  $\text{Er}^{3+}$  ions in  $\text{SiO}_2$ .<sup>9</sup> Investigations of time-resolved (TR) photoluminescence (PL) of  $\text{Er}^{3+}$  ions in  $\text{SiO}_2$ :SiNC reveal two major excitation mechanisms leading to 1.5  $\mu\text{m}$  emission, distinguishable by their dynamics: a fast one, taking  $\text{Er}^{3+}$  ions directly to the first excited state, and a slow one, exciting  $\text{Er}^{3+}$  ions to higher states ( $^4I_{11/2}$  or  $^4I_{9/2}$ ), followed by relaxation to  $^4I_{13/2}$  on a microsecond time scale.<sup>10–12</sup> The most direct evidence for the coexistence of the two excitation mechanisms has been found from investigations on the quantum efficiency of Er-related PL in the Er-SiNC system.<sup>13</sup>

Detailed investigation of the dynamics of 1.5  $\mu\text{m}$  PL emission shows three different regimes: (i) in times shorter than 1  $\mu\text{s}$ , an intense emission appears instantaneously after the laser pulse and rapidly decays toward a temporary minimum; (ii) there is then a slow temporal rise of PL on a microsecond time scale; (iii) there is a final slow decay on a millisecond time

scale.<sup>12,14,15</sup> While the slow rise and decay—regimes (ii) and (iii)—are conclusively assigned to the emission from  $^4I_{13/2}$  state of  $\text{Er}^{3+}$  ions, which is populated through higher excited states ( $^4I_{11/2}$  or  $^4I_{9/2}$ ), different explanations have been put forward for the 1.5  $\mu\text{m}$  emission in regime (i). It has been suggested that in high-temperature annealed samples of  $\text{SiO}_2$  doped with both  $\text{Er}^{3+}$  ions and SiNCs, a fast cooling of hot excitons created in SiNCs can be facilitated by an Auger process of energy transfer to  $\text{Er}^{3+}$  ions, which are then excited directly to the first  $^4I_{13/2}$  excited state on a nanosecond time scale. However, parallel to the fast excitation process, fast quenching takes place in which carriers confined in a SiNC acquire energy while bringing the excited  $\text{Er}^{3+}$  ions back to the ground state. As a result, intense Er-related emission appears and quenches within the first microsecond after laser pulse.<sup>12</sup> This interpretation has been challenged on the basis that a similar fast PL at 1.5  $\mu\text{m}$  was also observed in Er-free  $\text{SiO}_2$ :SiNC samples.<sup>15–17</sup> Therefore it has been postulated that the fast PL at 1.5  $\mu\text{m}$  arises due to deep trap centers which emit in the visible and infrared regions.<sup>15</sup> Following yet another interpretation, the fast infrared emission is related to recombination at defect centers either in the  $\text{SiO}_2$  matrix or at the interface with the SiNCs.<sup>16,17</sup> Therefore the origin of the fast 1.5  $\mu\text{m}$  emission—regime (i)—and the related energy transfer mechanism are still under debate.

The purpose of this study is to address the above-mentioned issues and resolve the origin of the 1.5  $\mu\text{m}$  submicrosecond emission. For this we have investigated the time and temperature dependence of 1.5  $\mu\text{m}$  emission from purposefully prepared  $\text{SiO}_2$ :SiNCs samples with and without  $\text{Er}^{3+}$  ions. The behavior of the PL dynamics for wavelengths other than that of Er-related emission (in this case 1.4  $\mu\text{m}$ ) has also been investigated. On the basis of this study we confirm that in the investigated materials the fast PL at 1.5  $\mu\text{m}$  is related to emission from  $\text{Er}^{3+}$  ions.

### II. EXPERIMENTAL DETAILS

The investigated 2- $\mu\text{m}$ -thick layers containing just SiNCs in  $\text{SiO}_2$  or codoped with  $\text{Er}^{3+}$  ions have been fabricated by the radio frequency cosputtering technique. The sputtering procedure was followed by annealing for 30 min in  $\text{N}_2$

atmosphere at 1150 °C. Further details of sample preparation can be found elsewhere.<sup>4</sup> The PL experiments were performed under pulsed excitation in the visible spectral range, provided by a tunable optical parametric oscillator pumped by the third harmonic of a Nd:YAG laser (where YAG indicates yttrium aluminum garnet), with pulse duration of 5 ns and repetition rate of 20 Hz. The samples were placed on the cold finger of a closed-cycle cryostat and measurements were taken at temperatures ranging from 7 to 300 K. PL spectra were resolved with a TRIAX 320 spectrometer and detected with an InGaAs photomultiplier tube (Hamamatsu R5509-72). For TR measurements of PL dynamics, the photomultiplier tube was working in time-correlated single-photon-counting mode. The overall temporal resolution of the experiments was limited by the laser pulse to  $\sim 5$  ns.

### III. RESULTS AND DISCUSSION

Figure 1 shows the PL spectra of the sample with  $\text{Er}^{3+}$  ions at room temperature (RT) and at  $T = 7$  K. The measurements were performed under excitation at  $\lambda_{exc} = 450$  nm (2.75 eV), i.e., not in resonance with any internal transition of  $\text{Er}^{3+}$  ions. SiNC- and Er-related bands can be seen around 0.9 and 1.5  $\mu\text{m}$ , respectively. In addition, at low temperature a third broad band peaking at 1.3  $\mu\text{m}$  can also be distinguished, having a nanosecond decay time constant; consequently its time-integrated intensity is small when compared to the other two bands. Similar emission around 1.3  $\mu\text{m}$  has been observed in the past and is usually identified as recombination at defects.<sup>18–22</sup> In the present case, this defect band becomes relevant due to the fact that its shoulder at longer wavelengths might overlap with the 1.5  $\mu\text{m}$  Er-related emission. At RT, the Er-related band broadens while its wavelength-integrated intensity remains practically constant. This could be due to population of upper states of the crystal-field-split multiplets of  $\text{Er}^{3+}$  ions.<sup>14</sup> We also note that the higher-energy side of the

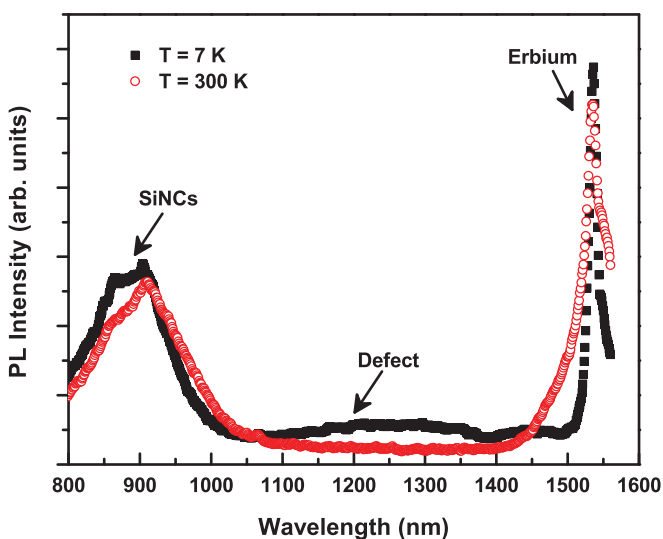


FIG. 1. (Color online) Time-integrated PL spectra at  $T = 7$  and 300 K, excited at  $\lambda_{exc} = 450$  nm. SiNC- and Er-related bands can be observed at  $T = 300$  K. In addition, at  $T = 7$  K a third broad band can be seen centered around 1.3  $\mu\text{m}$ .

SiNC-related band suffers from strong temperature quenching. This high-energy shoulder has been observed before and is believed to arise due to hot carrier recombination from higher electron (and/or hole) levels of SiNCs.<sup>14</sup>

The results of TR-PL from Er-doped and Er-free samples are summarized in Fig. 2. Figures 2(a)–2(c) compare the Er-doped and Er-free sample at RT while Figs. 2(d)–2(f) compare the same at  $T = 7$  K. Strong emission at 1.5  $\mu\text{m}$  is clearly observed in the Er-doped sample at both temperatures while there is no such signal in the Er-free sample. A defect-related signal is observed in both Er-doped and Er-free samples but only at low temperature. In order to allow for direct comparison with previous studies (Refs. 15 and 16), the wavelength dependence of the PL signals from Er-doped and Er-free samples integrated over a 0–200 ns time window is shown in Figs. 2(c) and 2(f). Here the SiNC-related emission band can also be seen in both samples, while the 1.5  $\mu\text{m}$  emission is present exclusively in the Er-doped sample.

Now we turn our attention to possible overlap between the defect- and Er-related PL bands. In order to investigate this we have examined two different approaches. First, we considered that the defect-related band has the same origin in the Er-doped and Er-free samples. Therefore, we compared the PL dynamics at 1.5  $\mu\text{m}$  from both samples. Results for  $T = 7$  and 300 K are shown in Figs. 3(a) and 3(b). The dynamics are then scaled according to their intensity ratio in the PL spectra. Afterward the scaled PL signal at 1.5  $\mu\text{m}$  from Er-free sample is subtracted from the Er-doped sample. This has been done for temperatures between 7 and 300 K, and the results are shown in Fig. 3(c). We conclude that after subtraction there remains a fast signal at 1.5  $\mu\text{m}$  which can now be assigned to emission from the first excited  $^4I_{13/2}$  state of  $\text{Er}^{3+}$  ions. As a side product of this data treatment we have also estimated the percentage of defect-related PL that might contribute to the total PL at 1.5  $\mu\text{m}$  in our material as not more than 24%.

In the second approach we considered that the defect-related emission can be modified due to the presence of  $\text{Er}^{3+}$  ions. For this we first analyze the PL dynamics from the Er-doped sample at 1.4  $\mu\text{m}$ , which is outside the range where the Er-related emission due to the  $^4I_{13/2} \rightarrow ^4I_{15/2}$  transition appears. Figures 4(a) and 4(b) compare the PL dynamics at 1.4 and 1.5  $\mu\text{m}$  for RT and  $T = 7$  K from the Er-doped sample. Both PL signals detected at 1.4 and 1.5  $\mu\text{m}$ , show the fast nanosecond time decay, slowing down with decreasing temperature. In order to remove the possible contribution of defect emission from the Er-related PL, we carefully subtracted the 1.4  $\mu\text{m}$  dynamics from the 1.5  $\mu\text{m}$  dynamics, extending the procedure over the temperature range between 7 and 300 K, as shown in Fig. 4(c). The data have been normalized and subtracted in such a way that after subtraction, the remaining signal has positive amplitude for the whole dynamical range. In this way we possibly subtracted too much of the signal but never too little. As can be seen, after the subtraction procedure we are again left with a strong fast nanosecond signal. We also calculated the percentage of 1.4  $\mu\text{m}$  defect-related PL that might contribute to the band at 1.5  $\mu\text{m}$  and this is not more than 40%. Hence, using two different approaches we conclude that in our study the main part of the fast emission at 1.5  $\mu\text{m}$  is Er-related. As a result of this data treatment the rise of the slow 1.5  $\mu\text{m}$  signal [region (ii)], believed to result

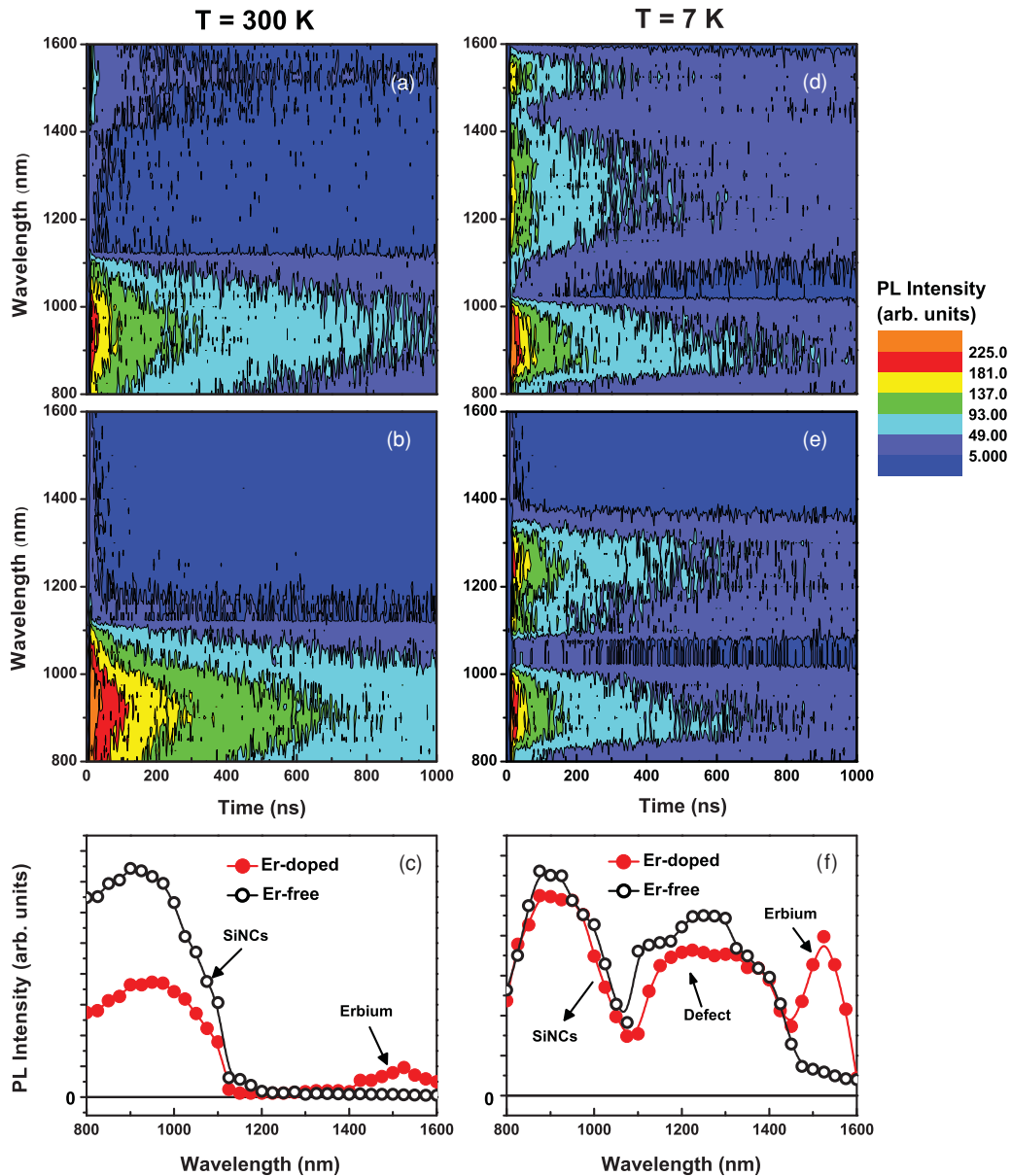


FIG. 2. (Color online) Time-resolved PL spectra at RT (a),(b),(c) and  $T = 7$  K (d),(e),(f) for Er-doped (a),(d) and Er-free (b),(e) samples. The PL intensity (colored contour plots) is represented as a function of time ( $x$  axis) and detection wavelength ( $y$  axis). The results show the PL decay in the first 1000 ns after laser excitation at  $\lambda_{exc} = 450$  nm. SiNC- and Er-related bands can be seen at both temperatures, while a broad band around  $\lambda_{exc} = 1.3 \mu\text{m}$  can only be observed at  $T = 7$  K. The spectral dependence of the integrated PL (0 to 200 ns) is compared for samples with and without  $\text{Er}^{3+}$  ions at RT (c) and at  $T = 7$  K (f).

from transitions from higher states of  $\text{Er}^{3+}$  ions, also becomes distinguishable [Fig. 4(c)]. In a direct measurement at low temperatures, this rise cannot be seen as it is merged with the broad defect band. After the data treatment it emerges and can be followed over the entire temperature range.

We have therefore established that the fast PL at  $1.5 \mu\text{m}$  observed in this study is due to the  ${}^4I_{13/2} \rightarrow {}^4I_{15/2}$  transition in  $\text{Er}^{3+}$  ions, but the question remains of how it is possible for  $\text{Er}^{3+}$  PL to appear and decay within the first microsecond after the laser pulse. While the present study does not conclusively resolve this issue, two possible mechanisms satisfy the condition that  $\text{Er}^{3+}$  ions rapidly attain the first excited  ${}^4I_{13/2}$  state.

(i) For  $\text{Er}^{3+}$  ions outside the SiNCs in the  $\text{SiO}_2$  matrix, an Auger-like process can transfer excess energy of hot carriers from SiNCs to nearby  $\text{Er}^{3+}$  ions. Up to  $\sim 50\%$  of all  $\text{Er}^{3+}$  content is in the effective range of this interaction.<sup>12,14</sup> Fast deexcitation of these  $\text{Er}^{3+}$  ions can take place by a reverse process, in which the energy is transferred back to carriers confined in the NCs. When the involved transition does not match the energy conservation requirements, this process must be phonon assisted,<sup>14</sup> which will manifest itself by characteristic temperature dependence of the decay time constant.

(ii)  $\text{Er}^{3+}$  ions inside the SiNCs or trapped at the SiNC/ $\text{SiO}_2$  boundary are susceptible to an instantaneous excitation

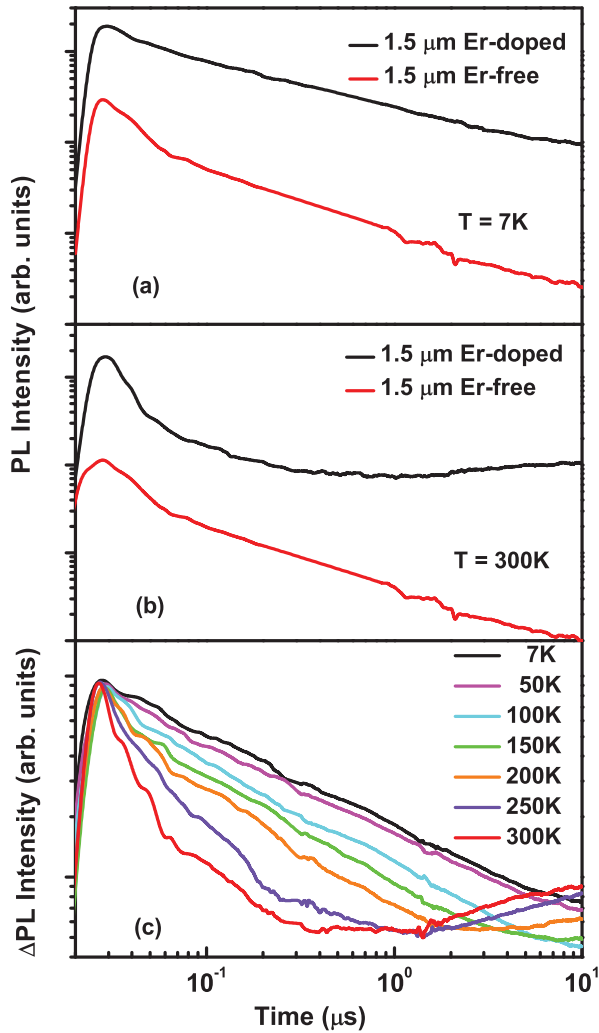


FIG. 3. (Color online) Comparison of time-dependent PL at  $1.5 \mu\text{m}$  from Er-free and Er-doped sample under pulsed excitation at  $\lambda_{exc} = 450 \text{ nm}$ . (a)  $T = 7 \text{ K}$  and (b)  $T = 300 \text{ K}$ . (c) Dynamics of the  $1.5 \mu\text{m}$  PL signal for Er-doped sample corrected with that observed for Er-free sample in 7–300 K temperature range. See text for details.

directly into the first excited state via direct absorption of photons with sufficient energy to excite erbium and create an electron-hole pair in the NC.<sup>14</sup> These  $\text{Er}^{3+}$  ions located in the NC can induce a donor center, as a result of which they will deexcite nonradiatively very fast, as observed also in bulk Si:Er.<sup>23</sup>

We have observed from Figs. 3(c) and 4(c) that the PL signal is quenched with temperature increase. Previous studies have shown that the activation energy derived from the temperature dependence of the PL intensity can give information on the microscopic mechanism responsible for this quenching.<sup>24–26</sup> We have observed that the PL signal from the defect-related band at  $1.4 \mu\text{m}$  is also quenched with temperature. Therefore, the microscopic origin of the defect- and Er-related bands can be distinguished if we determine the activation energies of the two bands. For this we have integrated the PL intensity over the first 200 ns for the  $1.5 \mu\text{m}$  and  $1.4 \mu\text{m}$  bands from the Er-doped sample and plotted it against temperature (Fig. 5). A

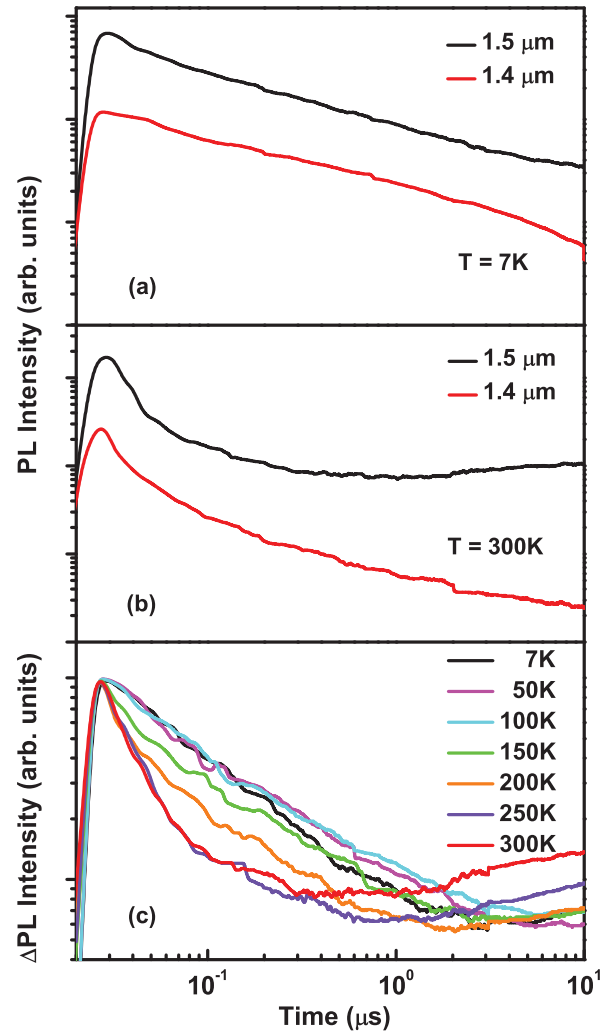


FIG. 4. (Color online) Comparison of the time-dependent PL at  $1.5$  and  $1.4 \mu\text{m}$  from Er-doped sample under pulsed excitation at  $\lambda_{exc} = 450 \text{ nm}$ . (a)  $T = 7 \text{ K}$  and (b)  $T = 300 \text{ K}$ . (c) Dynamics of the  $1.5 \mu\text{m}$  PL signal for Er-doped sample corrected with the  $1.4 \mu\text{m}$  PL signal from the same sample in 7–300 K temperature range. See text for details.

fit of the Arrhenius equation (dotted line in Fig. 5) gives the activation energy for the two bands, which is  $E_A \approx 60 \text{ meV}$  for the  $1.5 \mu\text{m}$  band and  $E_A \approx 90 \text{ meV}$  for the  $1.4 \mu\text{m}$  band. Therefore, we conclude that different centers are responsible for the thermal quenching of Er-related and defect-related PL bands, which serves as an independent proof of their different origin.

At this point, we suggest that there exist Er-related trap levels with ionization energy of  $60 \text{ meV}$ .<sup>27,28</sup> These trap levels are responsible for efficient excitation of  $\text{Er}^{3+}$  ions into the first excited state, while the reverse process takes the  $\text{Er}^{3+}$  ions back to the ground state. Thermally induced ionization of these trap levels is responsible for the observed temperature quenching. It is also possible that  $\text{Er}^{3+}$  ions placed outside SiNCs give the standard slow rise (microsecond) and decay (millisecond) of the PL signal, while only the  $\text{Er}^{3+}$  ions located inside SiNCs contribute to the the fast process.

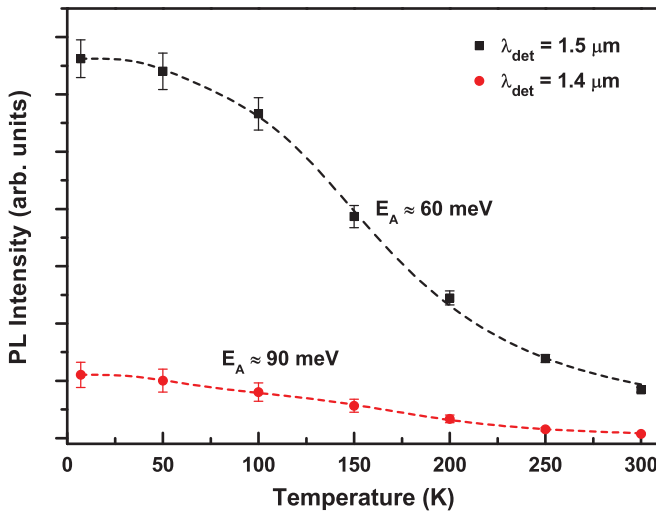


FIG. 5. (Color online) PL intensity of 1.5 and 1.4  $\mu\text{m}$  emission as a function of sample temperature. Dotted line shows the data fitting by the Arrhenius law. Activation energies of  $E_A \approx 60$  meV for 1.5  $\mu\text{m}$  and  $E_A \approx 90$  meV for 1.4  $\mu\text{m}$  emissions are found.

#### IV. CONCLUSION

We have shown that for the high-temperature-annealed SiNCs investigated in this study the major part of the fast PL at 1.5  $\mu\text{m}$  originates from the radiative  ${}^4I_{13/2} \rightarrow {}^4I_{15/2}$  transition of  $\text{Er}^{3+}$  ions. The activation energy of 60 meV derived from thermally induced quenching of this PL band shows that there are Er-related trap centers which are responsible for the fast rise and fast decay of the 1.5  $\mu\text{m}$  signal. The fast signal might also be related to  $\text{Er}^{3+}$  ions located inside the SiNC cores, where excitation and deexcitation become very efficient. These results offer additional insights for the understanding of Er-related energy transfer mechanisms in sensitized matrices.

#### ACKNOWLEDGMENTS

This work has been financially supported by Stichting voor de Technologische Wetenschappen (STW) and Nederlandse Organisatie voor Wetenschappelijk Onderzoek (NWO). S.S. acknowledges also the Higher Education Commission, Pakistan for an individual grant.

\*s.saeed@uva.nl

- <sup>1</sup>O. B. Gusev, M. S. Bresler, P. E. Pak, I. N. Yassievich, M. Forcales, N. Q. Vinh, and T. Gregorkiewicz, *Phys. Rev. B* **64**, 075302 (2001).
- <sup>2</sup>N. Q. Vinh, N. N. Ha, and T. Gregorkiewicz, *Proc. IEEE* **79**, 1269 (2007).
- <sup>3</sup>A. J. Kenyon, P. F. Trwoga, M. Federighi, and C. W. Pitt, *J. Phys.: Condens. Matter* **6**, L319 (1994).
- <sup>4</sup>M. Fujii, M. Yoshida, Y. Kanzawa, S. Hayashi, and K. Yamamoto, *Appl. Phys. Lett.* **71**, 1198 (1997).
- <sup>5</sup>M. Wojdak, M. Klik, M. Forcales, O. B. Gusev, T. Gregorkiewicz, D. Pacifici, G. Franzo, F. Priolo, and F. Iacona, *Phys. Rev. B* **69**, 233315 (2004).
- <sup>6</sup>F. Iacona, D. Pacifici, A. Irrera, M. Miritello, G. Franzo, F. Priolo, D. Sanfilippo, G. Di Stefano, and P. G. Fallica, *Appl. Phys. Lett.* **81**, 3242 (2002).
- <sup>7</sup>M. Schmidt, J. Heitmann, R. Scholz, and M. Zacharias, *J. Non-Cryst. Solids* **299**, 678 (2002).
- <sup>8</sup>D. Kovalev, J. Diener, H. Heckler, G. Polisski, N. Kunzner, and F. Koch, *Phys. Rev. B* **61**, 4485 (2000).
- <sup>9</sup>A. J. Kenyon, C. E. Chryssou, C. W. Pitt, T. Shimizu Iwayama, D. E. Hole, N. Sharma, and C. J. Humphreys, *J. Appl. Phys.* **91**, 367 (2002).
- <sup>10</sup>M. Fujii, K. Imakita, K. Watanabe, and S. Hayashi, *J. Appl. Phys.* **95**, 272 (2004).
- <sup>11</sup>O. Savchyn, R. M. Todi, K. R. Coffey, and P. G. Kik, *Appl. Phys. Lett.* **94**, 241115 (2009).
- <sup>12</sup>I. Izeddin, A. S. Moskalenko, I. N. Yassievich, M. Fujii, and T. Gregorkiewicz, *Phys. Rev. Lett.* **97**, 207401 (2006).
- <sup>13</sup>D. Timmerman, I. Izeddin, P. Stallinga, I. N. Yassievich, and T. Gregorkiewicz, *Nature Photon.* **2**, 105 (2008).
- <sup>14</sup>I. Izeddin, D. Timmerman, T. Gregorkiewicz, A. S. Moskalenko, A. A. Prokofiev, I. N. Yassievich, and M. Fujii, *Phys. Rev. B* **78**, 035327 (2008).

- <sup>15</sup>A. Al Choueiry, A. M. Jurdyc, B. Jacquier, F. Gourbilleau, and R. Rizk, *J. Appl. Phys.* **106**, 053107 (2009).
- <sup>16</sup>D. Navarro-Urrios, A. Pitanti, N. Daldosso, F. Gourbilleau, R. Rizk, B. Garrido, and L. Pavesi, *Phys. Rev. B* **79**, 193312 (2009).
- <sup>17</sup>A. Pitanti, D. Navarro-Urrios, N. Prtljaga, N. Daldosso, F. Gourbilleau, R. Rizk, B. Garrido, and L. Pavesi, *J. Appl. Phys.* **108**, 053518 (2010).
- <sup>18</sup>A. Kanjilal, L. Rebohle, S. Prucnal, M. Voelskow, W. Skorupa, and M. Helm, *Phys. Rev. B* **80**, 241313 (2009).
- <sup>19</sup>H. Elhouichet and M. Oueslati, *Phys. Status Solidi A* **204**, 1497 (2007).
- <sup>20</sup>A. A. Shklyaev, Y. Nakamura, and M. Ichikawa, *J. Appl. Phys.* **101**, 033532 (2007).
- <sup>21</sup>J. Schafer, A. P. Young, L. J. Brillson, H. Niimi, and G. Lucovsky, *Appl. Phys. Lett.* **73**, 791 (1998).
- <sup>22</sup>W. Fuhs, I. Ulber, G. Weiser, M. S. Bresler, O. B. Gusev, A. N. Kuznetsov, V. K. Kudoyarova, E. I. Terukov, and I. N. Yassievich, *Phys. Rev. B* **56**, 9545 (1997).
- <sup>23</sup>A. A. Prokofiev, I. N. Yassievich, H. Vrielinck, and T. Gregorkiewicz, *Phys. Rev. B* **72**, 045214 (2005).
- <sup>24</sup>S. Coffa, G. Franzo, F. Priolo, A. Polman, and R. Serna, *Phys. Rev. B* **49**, 16313 (1994).
- <sup>25</sup>F. Priolo, G. Franzo, S. Coffa, and A. Carnera, *Phys. Rev. B* **57**, 4443 (1998).
- <sup>26</sup>M. S. Bresler, O. B. Gusev, N. A. Sobolev, E. I. Terukov, I. N. Yassievich, B. P. Zakharchenya, and T. Gregorkiewicz, *Phys. Solid State* **41**, 770 (1999).
- <sup>27</sup>T. Gregorkiewicz, D. T. X. Thao, and J. M. Langer, *Appl. Phys. Lett.* **75**, 4121 (1999).
- <sup>28</sup>M. Forcales, T. Gregorkiewicz, I. V. Bradley and J-P. R. Wells, *Phys. Rev. B* **65**, 195208 (2002).